

# Influence of Temperature and Relative Humidity on the Atmospheric Corrosion of Zinc in Field Exposures and Laboratory Environments by Atmospheric Corrosion Monitor

Xiaoming Wang<sup>1</sup>, Xingeng Li<sup>2</sup>, Xuelei Tian<sup>1,\*</sup>

<sup>1</sup> Key Laboratory for Liquid-Solid Structural Evolution and Processing of Materials (Ministry of Education), School of Materials Science and Engineering, Shandong University, Jinan 250061, China

<sup>2</sup> Shandong Electric Power Research Institute, Jinan 250001, China

\*E-mail: [tianxl\\_sdu@126.com](mailto:tianxl_sdu@126.com)

Received: 27 June 2015 / Accepted: 22 July 2015 / Published: 26 August 2015

---

In the present work, the effect of temperature and relative humidity on the corrosion rate of zinc in field exposures for nearly one year or in laboratory corrosion environments was investigated by zinc-graphite coupling type atmospheric corrosion monitor (ACM) sensor. During the field exposure, the temperature, relative humidity and corrosion rate were monitored continuously at the same time. The results showed that using the time of wetness (TOW) alone to estimate the corrosion rate of zinc had some limitations. To address this problem, ACM was also used in laboratory corrosion tests, which were performed in the chamber with controlled temperature and humidity. It was found that both temperature and relative humidity could affect the corrosion rate of zinc, and there was a coupling effect between the temperature and relative humidity on the corrosion rate. Based on the data from the laboratory corrosion tests, a new equation was proposed to describe the correlation of corrosion rate with temperature and relative humidity, which also considered the coupling effect between temperature and relative humidity. This equation better reflected the atmospheric corrosion rate of Zn during field exposures compared to the TOW.

---

**Keywords:** Atmospheric corrosion; Zinc; Atmospheric corrosion monitor; Temperature; Humidity

## 1. INTRODUCTION

Zinc (Zn) has been extensively used as coatings, paint pigments and sacrificial anodes to protect metals against corrosion because of its relatively low corrosion potential in the electrochemical series and low price [1-4]. Since many metallic materials and structures are exposed to atmospheric environments, the atmospheric corrosion of Zn has received considerable interest [1,2,5,6]. The

atmospheric corrosion is one of the most common degradation processes of metallic materials, which can cause significant damage to infrastructures [1,7-15]. The atmospheric corrosion of metals is a complex process that involves the chemical, electrochemical, and physical processes in solid, liquid, and gas phases [16,17]. In contrast to the corrosion process that happens in the bulk aqueous solution, the atmospheric corrosion generally occurs under a thin electrolyte layer on the metal surface and such layer can be formed in various conditions such as dew, rainfall, melting snow and water condensation in high humidity atmospheres [5,18-21].

The atmospheric corrosion of Zn has been extensively investigated in field exposures and in laboratory under controlled environments [2,22-25]. Field exposures have the benefits of reflecting the corrosion process in the real world. In order to guide the safe usage and predict the performance of metals in field exposures, it is rather important to investigate the relationship between the corrosion rate and the environmental factors such as relative humidity (RH), wet-dry cycles and temperature. It has been generally accepted that the thin electrolyte layer on the metal surface plays an important role in the corrosion process, which is highly dependent on the environmental characteristics [1,3,26]. According to ISO 9223 [18], the period during which a metallic surface is covered by adsorptive and/or liquid film of electrolyte is defined as time of wetness (TOW), which determines the time of the electrochemical corrosion process and affects the mass transport during the electrochemical corrosion [26-28]. Although it has been widely reported that the TOW is strongly related with the initiation and progress of the atmospheric corrosion [26,27,29,30], the exact effect of environmental factors (e.g., RH and temperature) on the corrosion behavior and rate during field exposures is quite complicated [31-33]. Corvo et al. [33] observed that for temperatures higher than 25 °C the determination of TOW changed, and a significant diminution of the surface water layer took place when air temperature was over 25 °C. Mikhailov et al. [31] reported that the atmospheric corrosion rate increased with the increasing temperature in a range of lower temperatures below 10 °C while it decreased as the temperature increased in a range of higher temperatures above 10 °C. Morcillo et al. [32] found that the atmospheric corrosion of Zn could occur below 0 °C, and it was possible to measure the electrochemical activity on the metallic surface below the ice layer.

To date, the dependence of the corrosion rate on the RH and temperature remains unclear. In addition, among various approaches for investigating the atmospheric corrosion, the use of Atmospheric Corrosion Monitor (ACM) has been proposed as an effective method to study the corrosivity of metals in field exposures due to several distinct advantages such as quantitative, direct and automatic measurement of the corrosion rate [5,34]. However, there have been no reports on corrosion monitoring for Zn in field exposures using ACM.

In the present work, zinc-graphite coupling type ACM sensor was used to investigate the effect of temperature and relative humidity on the corrosion rate of Zn in field exposures for nearly one year and also in laboratory environments. During the atmospheric corrosion tests, the temperature, relative humidity and corrosion rate of Zn were monitored continuously by ACM at the same time. The coupling effect between the temperature and relative humidity on the corrosion rate of Zn was found. A new equation was proposed to describe the correlation of corrosion rate of Zn with temperature and relative humidity, and it could better reflect the atmospheric corrosion rate of Zn in field exposures compared to the TOW.

## 2. EXPERIMENTAL

### 2.1. Features of ACMs

Fig. 1 shows the schematic illustration of the Zn–Graphite coupling type ACM sensor developed by the Tianjin University–Liceram Joint Laboratory. The structure of the ACM sensor is in the sandwich form, and there is a porous insulating film (0.02 mm thick) between the tested Zn specimen and conductive graphite film. Because of the porous structure of the insulating film, when a thin water film is formed between Zn and graphite film due to the water condensation, rainfall and etc., a galvanic current passes between Zn and graphite. This galvanic current has been found to show a good relationship with the corrosion rate of metals [5,35]. Therefore, the corrosion process of Zn can be monitored by measuring the galvanic current. The fabricated ACM can also monitor the temperature and RH at the same time.

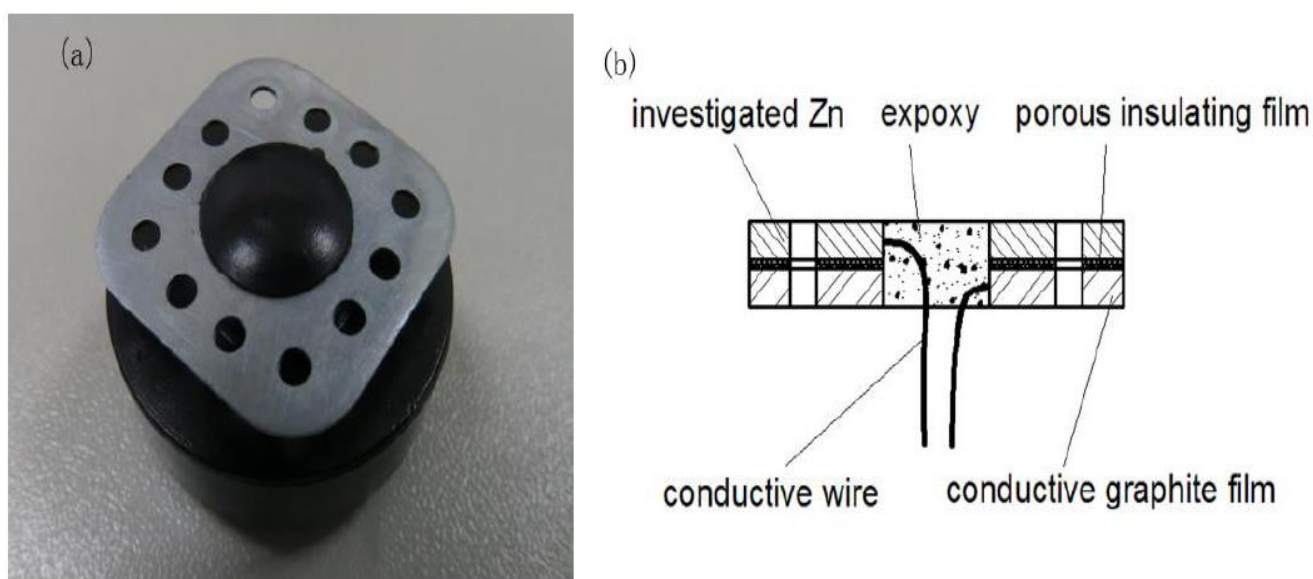


**Figure 1.** (a) Zn-graphite ACM sensor detecting the galvanic current used in the present work, and (b) the schematic diagram of the ACM sensor.

### 2.2. Field exposure test

Zn ACMs were mounted on exposure racks at an angle of  $45^\circ$  to the horizontal at 24 test stations in Shandong Province, China (Fig. 2). During the field exposure period, the galvanic current, RH and temperature were monitored by the ACM. The data was collected by the ACM every 10 minutes. Fig. 3 shows the photograph of the installed ACM for field exposure test in Jiaodong site.



**Figure 2.** Exposure sites in Shandong province, China.



**Figure 3.** The photograph of the ACM in field exposure in Jiaodong site.

2.3. Laboratory corrosion test

The Zn ACM was placed inside a chamber with controlled humidity or temperature, and the metal surface was at an angle of 45° to the horizontal. In the case of constant temperature tests, the temperature was set at as a constant value of 285, 300 and 308 K, and an alternating RH variation was subjected to the Zn ACM. For the constant temperature tests, the RH was set at as a constant value of 53%, 84%, and 92%, respectively. During the laboratory corrosion test, the galvanic current, actual RH and temperature in the chamber were monitored by the ACM.

3. RESULTS AND DISCUSSION

3.1. Field exposure tests

Fig. 4 shows the data of the temperature, RH, galvanic current, and charge quantity with time in field exposure test, which was measured in Shanxian site for one week. It is seen that the value of the temperature fluctuated remarkably between 293 and 311 K during day and night, and the RH value fluctuated between 28% and 94% with time. Correspondingly, the galvanic current varied with the changing temperature and RH. Previous studies found that the corrosion rate of metals has a good relationship with the galvanic current [5,22,36]. The charge quantity increased continuously with time as the corrosion process continued, indicating the increasing corrosion amount of Zn specimen with exposure time.

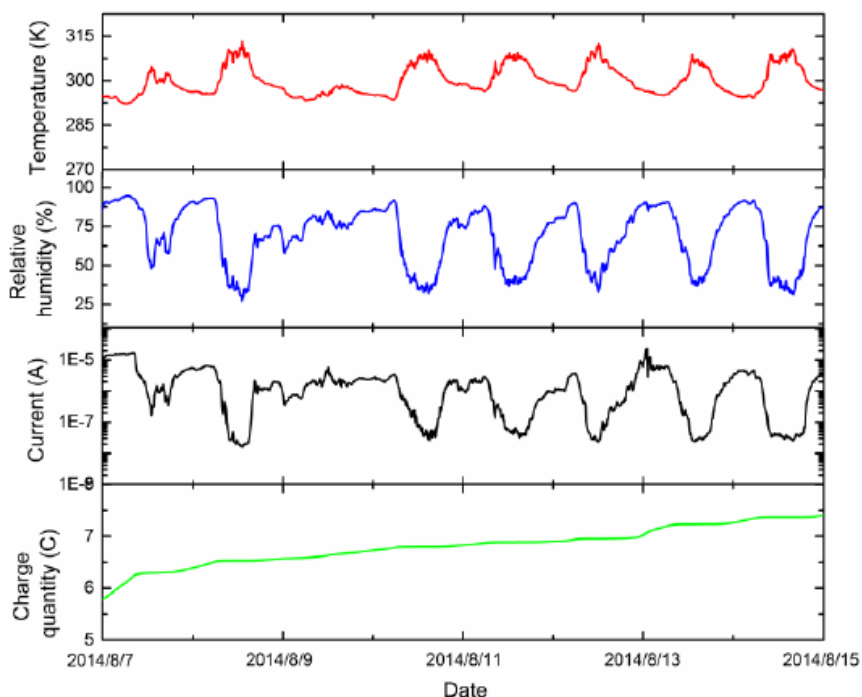
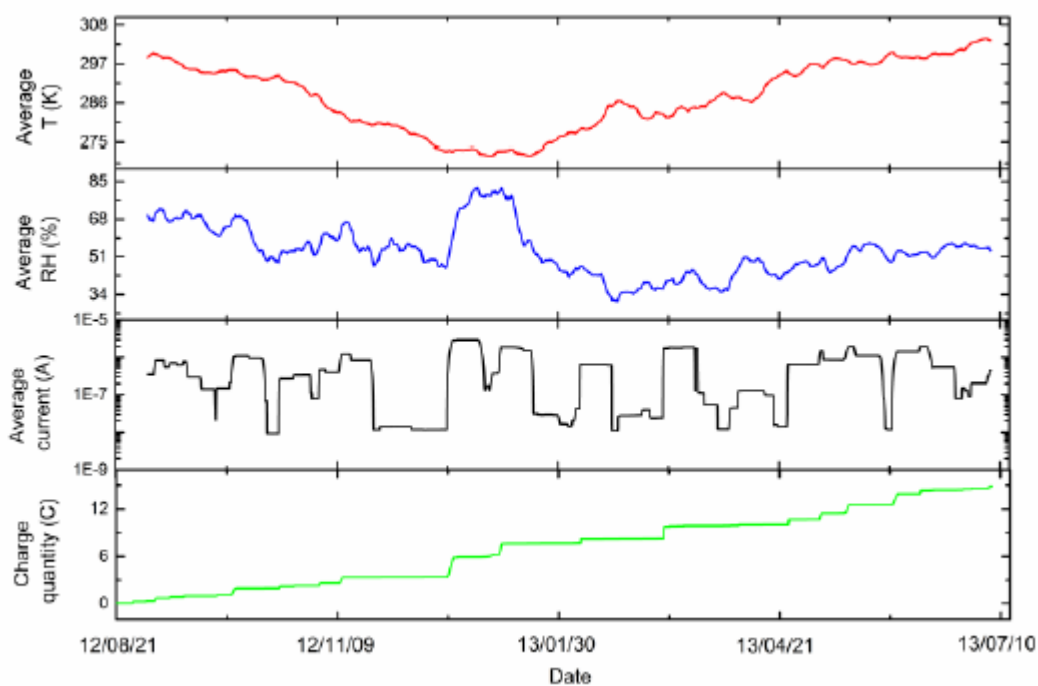


Figure 4. The monitored data of the temperature, RH, galvanic current and charge quantity by ACM in Shanxian site.

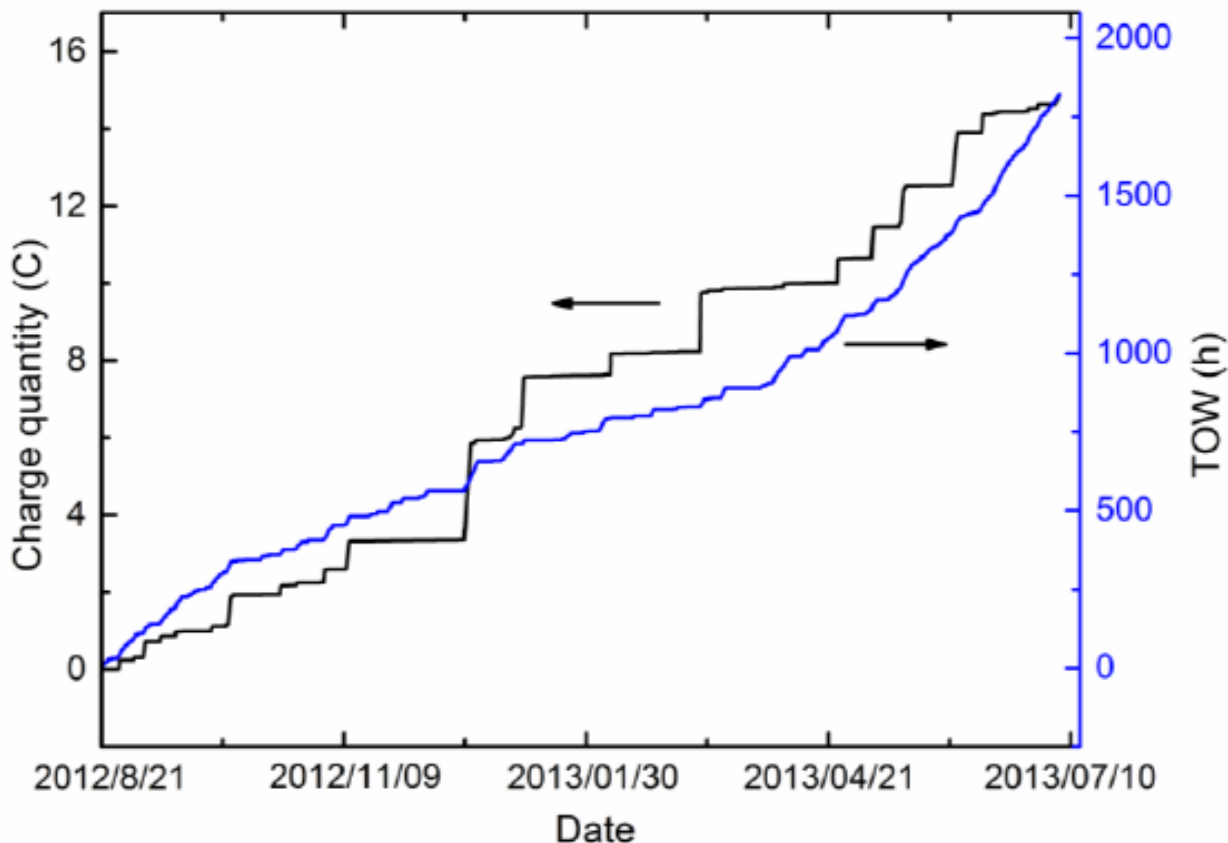
In order to demonstrate the long-term atmospheric corrosion data, Fig. 5 shows the change of the average temperature, average RH, average galvanic current, and charge quantity with time in Jinan site for nearly one year. Since the values of temperature, RH and galvanic current changed drastically from day to night, the data of them were averaged from 10 days. The temperature decreased from 300 to 271 K from Aug., 2012 to Dec., 2012. There is no obvious trend for the RH value and it was within the range between 30% and 82%. During the investigated exposure period, the highest galvanic current was  $2.8 \times 10^{-6}$  A, which was about two orders of magnitude higher than the lowest galvanic current. Generally, the change of the average galvanic current didn't follow the change of the temperature and RH, although they showed similar trend in some cases (e.g., from 15 Dec. to 28 Dec., 2012). As the atmospheric corrosion process proceeded, the charge quantity increased continuously with time.



**Figure 5.** The 10-day average data of the temperature, RH, galvanic current, and charge quantity for nearly one year in Jinan site.

Since TOW has been widely used to describe the development of the corrosion process of metals, Fig. 6 shows the change of the charge quantity and TOW with time in Jinan site for nearly one year. The value of TOW increased continuously with time. The charge quantity also increased with time, and there was several sudden increase of the charge quantity in the field exposure from Dec., 2012 to Mar., 2013. This feature was different with that of TOW curve. The above result suggests that using TOW to evaluate the corrosion content and rate has some limitations, which has also reported by the previous studies [16,21,34]. For example, Schindelholz et al. [28] pointed out that the inaccuracy of using TOW to evaluate the corrosion rate originated from a humidity threshold well above the

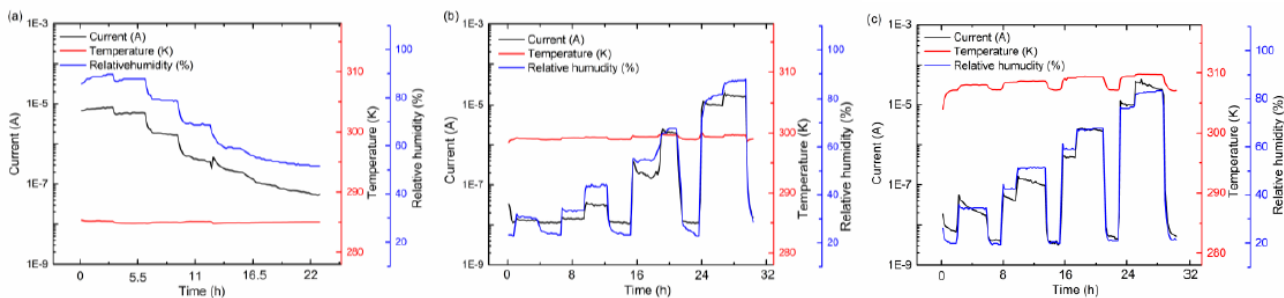
drying point of deposited aerosols and differences between surface and ambient RH. In an effort to solve this problem, laboratory corrosion tests was carried out in the present work.



**Figure 6.** The charge quantity and TOW measured by ACM in Jinan site for nearly one year.

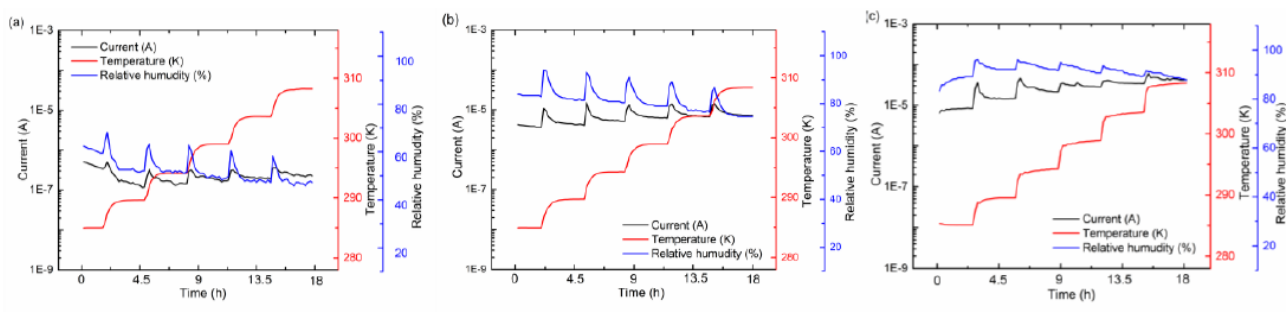
### 3.2. Laboratory corrosion tests

Fig. 7a–c show values of the galvanic current, temperature and RH measured by the Zn ACM in the test chamber, and the temperature was set at as a constant value of 285, 300 and 308 K, respectively. The tested Zn specimen in the chamber was subjected to an alternating RH variation. It is seen that the corrosion density was very sensitive to the change of the RH, and it almost changed instantaneously with the variation of the RH. Generally, for all the three investigated temperatures, the galvanic current increased with the increasing RH value. Many studies found that the RH played a critical role in the corrosion rate of metals, and the corrosion rate generally increased with the increasing RH [3,15,37-39].



**Figure 7.** The monitored galvanic current, temperature and RH by Zn ACM in the test chamber, with the temperature set as constant value of (a) 285 K, (b) 300 K, and (c) 308 K, respectively.

Fig. 8a–c show values of the galvanic current, temperature and RH measured by the Zn ACM in the test chamber, and the RH was set at as a constant value of 53%, 84%, and 92%, respectively. To further illustrate the RH effect on the galvanic current, a step-increase temperature up to 308 K was applied on the investigated Zn specimen. In this case, although the RH value was set at a constant value, the actual RH value (monitored by the ACM) could be changed rapidly during the initial stage of the temperature increase. Again, the value of the galvanic current changed rapidly with the change of the RH, and the galvanic current was raised as the RH increased.



**Figure 8.** The monitored galvanic current, temperature and RH by Zn ACM in the test chamber, with the RH set as constant value of (a) 53%, (b) 84%, and (c) 92%, respectively.

To clearly illustrate the effect of temperature and RH on the galvanic current, Fig. 9a shows the relationship between the galvanic current and RH under different temperatures, and the data was obtained from Fig. 7. It is seen that the logarithm of the galvanic current (*i*) was in linear relationship with the RH value:

$$\lg i = a + b \cdot RH \tag{1}$$

Fig. 9b shows the relationship between the galvanic current and temperature under different RH values, and the data was obtained from Fig. 8. Similarly, the logarithm of the galvanic current was in linear relationship with the temperature:

$$\lg i = c + d \cdot T \tag{2}$$

Table 1 shows the fitted value of slope  $b$  and  $d$  in equation (1) and (2), respectively. The value of slope  $b$  increased with the increasing temperature and that of slope  $d$  increased with the increasing RH, indicating that the temperature and RH had a coupling effect on galvanic current (i.e., corrosion rate). Although previous work found that the increasing temperature and RH could enhance the corrosion rate, the coupling effect between them has not been considered [3,15,37,38]. Considering the coupling effect between the temperature and RH, equations (1) and (2) can be written as equation (3) and (4), respectively:

$$lgi = (e_1 + a' \cdot T) + (e_2 + b' \cdot T) \cdot RH \tag{3}$$

$$lgi = (e_3 + c' \cdot RH) + (e_4 + d' \cdot RH) \cdot T \tag{4}$$

From equations (3) and (4), the relationship between the galvanic current, temperature and RH can be finally achieved as:

$$lgi = e_1 + e_4 \cdot T + e_2 \cdot RH + b' \cdot T \cdot RH \tag{5}$$

Based on the data fit in Fig. 9, the value of the constants in equation (5) was obtained and can be written as:

$$lgi = -10.2408 + 0.0019 \cdot T - 0.02933 \cdot RH + 0.0003 \cdot T \cdot RH \tag{6}$$

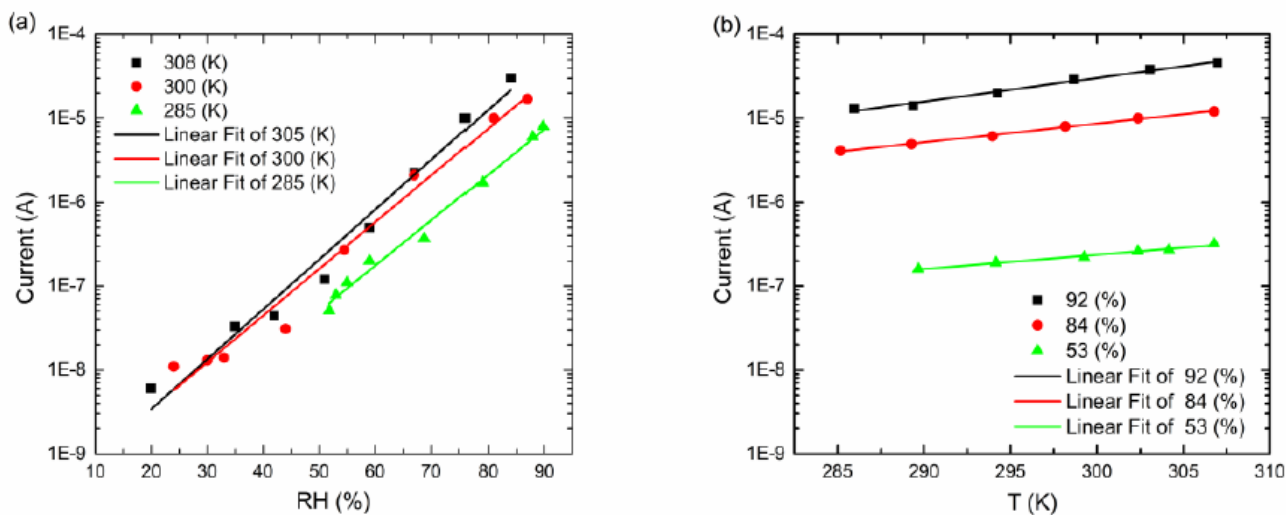


**Figure 9.** (a) Relationship and the linear fit between the galvanic current and RH under different temperatures, (b) relationship and the linear fit between the galvanic current and temperature under different RH

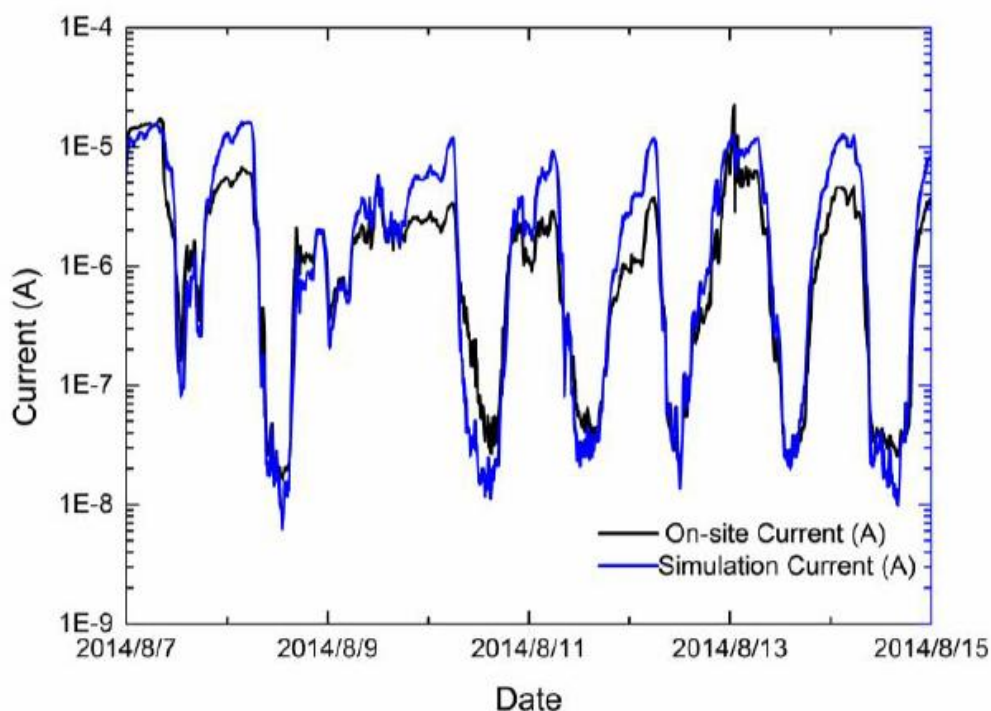
**Table 1.** The fitted results of the slope in equation (1) and (2)

Temperature (K)	Slope $b$ in equation (1)	RH (%)	Slope $d$ in equation (2)
285	0.0541	53	0.0170
300	0.0557	84	0.0223
308	0.0594	92	0.0281

### 3.3. Comparison between the simulated and actual data.

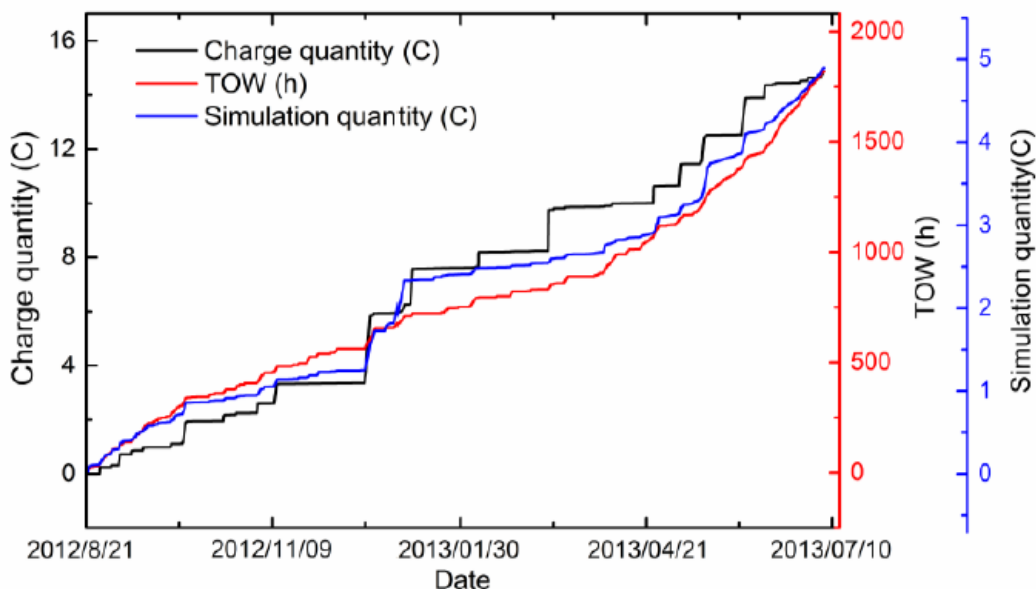
By substituting the  $T$  and  $RH$  in equation (6) with the actual values measured by ACM in the Shanxian site (Fig. 4), the simulated value of the galvanic current was obtained and compared with that monitored by ACM, as shown in Fig. 10. The simulated galvanic current agreed well with the actual galvanic current.

Fig. 11 shows compared the charge quantity of the monitored data by ACM (Fig. 6) and simulated data during nearly one-year field exposure in Jinan site. Compared to the TOW curve, the curve of the simulated charge quantity was closer to the charge quantity obtained by ACM. For example, from Dec., 2012 to Feb., 2013, the simulated charge quantity matched quite well with the monitored one whereas TOW failed to reflect the slow increase of the charge quantity from Nov. to Dec., 2012 and the quick increase of the charge quantity from Dec., 2012 to Feb., 2013. This is because that our model considered the combined effect of temperature and RH on the corrosion rate, and the corrosion in low temperatures (i.e., in winter season) was taken into account by our model.



**Figure 10.** The simulated galvanic current and the actual galvanic current obtained by ACM in field exposure in the Shanxian site.

This suggested that the model developed in the present work was more accurate to describe the development of corrosion process of Zn compared to TOW. It was also noted that in some cases, for example, from Mar. to May., 2013, both TOW and our model couldn't reflect well the corrosion process of Zn. This might be attributed to the reason that the effect of rain [26], snow, and pollutants [40-43] were not taken into account in the present work. Further work should be carried out to address this problem.



**Figure 11.** Comparison between the charge quantity of the monitored data by ACM and simulated data obtained in Jinan site.

#### 4. CONCLUSIONS

The effect of temperature and relative humidity on the atmospheric corrosion rate of zinc in field exposures for nearly one year or in laboratory corrosion environments was investigated by zinc-graphite type ACM sensor. The corrosion rate increased with the temperature (from 285 to 308 K) and RH (from 53% to 92%), and the RH had a larger influence on the corrosion rate compared to the temperature. Furthermore, the temperature and RH had a coupling effect on the corrosion rate of Zn. Using the time of wetness (TOW) alone to estimate the corrosion rate of zinc had some limitations. A new equation was proposed to describe the correlation of corrosion rate with temperature and RH, which also considered the coupling effect between temperature and RH. Compared to the TOW, the new equation developed in the present work better reflected the atmospheric corrosion rate of Zn during field exposures.

#### ACKNOWLEDGEMENTS

This work was supported by Shandong Electric Power Research Institute and Tianjin University–Liceram Joint Laboratory.

#### References

1. T.H. Muster, A. Bradbury, A. Trinchi, I.S. Cole, T. Markley, D. Lau, S. Dligatch, A. Bendavid, P. Martin, *Electrochimica Acta* 56 (2011) 1866.
2. A.P. Yadav, F. Suzuki, A. Nishikata, T. Tsuru, *Electrochimica Acta* 49 (2004) 2725.

3. Q. Cheng, S. Song, L. Song, B. Hou, *Journal of the Electrochemical Society* 160 (2013) C380.
4. S. Song, Z. Chen, *Journal of the Electrochemical Society* 161 (2014) C288.
5. X. Cao, H. Deng, W. Lan, P. Cao, *Anti-Corrosion Methods and Materials* 60 (2013) 199.
6. X. Zhao, S. Xing, J. Yang, J. Zhang, *International Journal of Electrochemical Science* 9 (2014) 5877.
7. S. Oesch, P. Heimgartner, *Materials and Corrosion* 47 (1996) 425.
8. C. Zhong, F. Liu, Y.T. Wu, J.J. Le, L. Liu, M.F. He, J.C. Zhu, W.B. Hu, *Journal of Alloys and Compounds* 520 (2012) 11.
9. R. Vera, S. Ossandon, *International Journal of Electrochemical Science* 9 (2014) 7131.
10. C. Zhong, M.F. He, L. Liu, Y.J. Chen, B. Shen, Y.T. Wu, Y.D. Deng, W.B. Hu, *Surface & Coatings Technology* 205 (2010) 2412.
11. H.C. Vasconcelos, B.M. Fernandez-Perez, J. Morales, R. M. Souto, S. Gonzalez, V. Cano, J. J. Santana, *International Journal of Electrochemical Science* 9 (2014) 6514.
12. C. Zhong, M.F. He, L. Liu, Y.T. Wu, Y.J. Chen, Y.D. Deng, B. Shen, W.B. Hu, *Journal of Alloys and Compounds* 504 (2010) 377.
13. J.J. Le, L. Liu, F. Liu, Y.D. Deng, C. Zhong, W.B. Hu, *Journal of Alloys and Compounds* 610 (2014) 173.
14. C. Zhong, W.B. Hu, Y.M. Jiang, B. Deng, J. Li, *Journal of Coatings Technology and Research* 8 (2011) 107.
15. C. Zhong, X. Tang, Y.F. Cheng, *Electrochimica Acta* 53 (2008) 4740.
16. J. Hedberg, S. Baldelli, C. Leygraf, *Journal of Physical Chemistry C* 113 (2009) 6169.
17. J. Tidblad, T.E. Graedel, *Corrosion Science* 38 (1996) 2201.
18. ISO 9223, Corrosion of metals and alloys - corrosivity of atmospheres - classification.
19. C. Zhong, W.B. Hu, Y.F. Cheng, *Journal of Power Sources* 196 (2011) 8064.
20. J. Liu, W.B. Hu, C. Zhong, Y.F. Cheng, *Journal of Power Sources* 223 (2013) 165.
21. C. Zhong, W.B. Hu, Y.F. Cheng, *Journal of Materials Chemistry A* 1 (2013) 3216.
22. Q. Qu, C.W. Yan, Y. Wan, C.N. Cao, *Corrosion Science* 44 (2002) 2789.
23. H. Katayama, S. Kuroda, *Corrosion Science* 76 (2013) 35.
24. D. Persson, T. Prosek, N. LeBozec, D. Thierry, G. Luckeneder, *Corrosion Science* 90 (2015) 276.
25. D. Persson, D. Thierry, N. LeBozec, T. Prosek, *Corrosion Science* 72 (2013) 54.
26. L. Veleva, M. Acosta, E. Meraz, *Corrosion Science* 51 (2009) 2055.
27. C. Li, Y. Ma, Y. Li, F. Wang, *Corrosion Science* 52 (2010) 3677.
28. E. Schindelholz, R.G. Kelly, I.S. Cole, W.D. Ganther, T.H. Muster, *Corrosion Science* 67 (2013) 233.
29. I.S. Cole, W.D. Ganther, S.A. Furman, T.H. Muster, A.K. Neufeld, *Corrosion Science* 52 (2010) 848.
30. L.T.H. Lien, P.T. San, H.L. Hong, *Science and Technology of Advanced Materials* 8 (2007) 552.
31. A.A. Mikhailov, J. Tidblad, V. Kucera, *Protection of Metals* 40 (2004) 601.
32. M. Morcillo, B. Chico, D. de la Fuente, E. Almeida, G. Joseph, S. Rivero, B. Rosales, *Cold Regions Science and Technology* 40 (2004) 165.
33. F. Corvo, T. Pérez, Y. Martin, J. Reyes, L.R. Dzib, J. González-Sánchez, A. Castañeda, *Corrosion Science* 50 (2008) 206.
34. D. Delgado, R. Vera, *International Journal of Electrochemical Science* 8 (2013) 7687.
35. D. Mizuno, S. Suzuki, S. Fujita, N. Hara, *Corrosion Science* 83 (2014) 217.
36. K. Fujii, K. Ohashi, T. Hashimoto, N. Hara, *Materials Transactions* 53 (2012) 412.
37. G.A. El-Mahdy, K.B. Kim, *Corrosion Science and Technology* 3 (2004) 251.
38. S.C. Chung, A.S. Lin, J.R. Chang, H.C. Shih, *Corrosion Science* 42 (2000) 1599.
39. R. Lindstrom, J.E. Svensson, L.G. Johansson, *Journal of the Electrochemical Society* 147 (2000) 1751.
40. R.E. Lobnig, D.J. Siconolfi, L. Psota-Kelty, G. Grundmeier, R.P. Frankenthal, Stratmann, M.

*Journal of the Electrochemical Society* 143 (1996) 1539.

41. H. Gil, C. Leygraf, J. Tidblad, *Journal of the Electrochemical Society* 159 (2012) C123.

42. J. Morales, F. Diaz, J. Hernandez-Borges, S. Gonzalez, V. Cano, *Corrosion Science* 49 (2007) 526.

43. F.J. Hernandez, J.J. Santana, R.M. Souto, S. Gonzalez, J. Morales, *International Journal of Electrochemical Science* 6 (2011) 6567.

© 2015 The Authors. Published by ESG ([www.electrochemsci.org](http://www.electrochemsci.org)). This article is an open access article distributed under the terms and conditions of the Creative Commons Attribution license (<http://creativecommons.org/licenses/by/4.0/>).